Bone 65 (2014) 33–41

Contents lists available at ScienceDirect

Bone

journal homepage: www.elsevier.com/locate/bone

Original Full Length Article

Gene expression profile induced by ovariectomy in bone marrow of mice: A functional approach to identify new candidate genes associated to osteoporosis risk in women

Begoña Pineda [a], Eva Serna [b], Andrés Laguna-Fernández [c], Inmaculada Noguera [b], Layla Panach [a], Carlos Hermenegildo [a,c], Juan J. Tarín [d], Antonio Cano [e], Miguel Ángel García-Pérez [a,f,*]

[a] Research Foundation, Institute of Health Research INCLIVA, Valencia, Spain
[b] Research Unit — INCLIVA, Faculty of Medicine, University of Valencia, Spain
[c] Department of Physiology, University of Valencia, Spain
[d] Department of Functional Biology and Physical Anthropology, University of Valencia, Spain
[e] Department of Pediatrics, Obstetrics and Gynecology, University of Valencia, Spain
[f] Department of Genetics, University of Valencia, Spain

ARTICLE INFO

Article history:
Received 4 October 2013
Revised 16 April 2014
Accepted 1 May 2014
Available online 9 May 2014

Edited by: Bente Langdahl

Keywords:
Association studies
Translational research
Ovariectomy
Bone marrow
CD79A
GPX3 genes

ABSTRACT

Osteoporosis is a multifactorial skeletal pathology with a main genetic component. To date, however, the majority of genes associated with this pathology remain unknown since genes cataloged to date only explain a part of the heritability of bone phenotypes. In the present study, we have used a genome-wide gene expression approach by means of microarrays to identify new candidate genes involved in the physiopathology of osteoporosis, using as a model the ovariectomized (OVX) mice by comparing global bone marrow gene expression of the OVX mice with those of SHAM operated mice. One hundred and eighty transcripts were found to be differentially expressed between groups. The analysis showed 23 significant regulatory networks, of which the top five canonical pathways included B-cell development, primary immunodeficiency signaling, PI3K signaling in B-cells, phospholipase C signaling, and FcgRIIB signaling in B-cells. Twelve differentially expressed genes were validated by MALDI-TOF mass spectrometry with good reproducibility. Finally, the association to bone phenotypes of SNPs in genes whose expression was increased (*IL7R* and *CD79A*) or decreased (*GPX3* and *IRAK3*) by OVX in mice was analyzed in a cohort of 706 postmenopausal women. We detected an association of a SNP in a gene involved in the detoxification of free radicals like glutathione peroxidase 3 (*GPX3*) with femoral neck BMD (rs8177447, $P = 0.043$) and two SNPs in the Ig-alpha protein of the B-cell antigen component gene (*CD79A*) with lumbar spine BMD (rs3810153 and rs1428922, $P = 0.016$ and $P = 0.001$, respectively). These results reinforce the role of antioxidant pathways and of B-cells in bone metabolism. Furthermore, it shows that a genome-wide gene expression approach in animal models is a useful method for detecting genes associated to BMD and osteoporosis risk in humans.

Introduction

The increased life expectancy that occurs not only in developed, but also in developing countries, has led to a higher incidence of degenerative disorders such as osteoporosis [1]. Osteoporosis is a common age-related systemic skeletal disease associated with low bone mineral density (BMD) and micro-architectural deterioration of bone tissue leading to an increased risk of bone-fragility fractures affecting both women and men [1]. Other features of this pathology are low bone mass, altered bone material composition and increased rates of bone remodeling. Among all these phenotypes, BMD is the best predictor of bone fracture, the major complication of osteoporosis that is responsible of the morbidity and mortality associated with this pathology [2].

Osteoporosis is a multifactorial disease and according to the WHO, the phenotype that defines it, BMD, is influenced by environmental, medical, genetic and also epigenetic factors [3]. Certainly, there is abundant evidence obtained from studies in twins, families and in epidemiological studies which reveal a significant genetic contribution to phenotypic variation in BMD. This is true as well in other phenotypes that are predictors of bone fracture, like skeletal geometry, bone turnover or the ultrasound properties of bone, with estimates of heritability ranging between 0.5 and 0.8 [4–6].

To find the underlying genes that regulate susceptibility to low bone mass and osteoporosis, different strategies have been used, including

* Corresponding author at: Department of Genetics, University of Valencia, C/Dr. Moliner, 50, 46100 Burjassot, Valencia, Spain. Fax: +34 96 386 48 15.
E-mail address: migarpe@uv.es (M.Á. García-Pérez).

http://dx.doi.org/10.1016/j.bone.2014.05.001
8756-3282/

linkage studies, studies of candidate genes with *a priori* hypotheses, hypothesis-free genome-wide association studies (GWAS), and functional studies [4]. Linkage studies, given the multifactorial nature of the common form of osteoporosis, are not the best approach to the study of this pathology because of the low penetrance of the character [7]. Thus, like other complex diseases, most reports have been *a priori* hypothesis association studies with candidate genes. This approach has focused mainly on genes regulating bone metabolism and cytokines whose implication in bone metabolism has been well-known for some time. For example, *ESR1*, *COL1A1*, *VDR*, *TGFB1*, *IL-6*, *TNF-α*, *OPG*, and *LRP5* represent some of the approximately 150 candidate genes that have been investigated [4]. Recently, given the advances in high-throughput genotyping methods, GWAS have been performed in thousands of people comprising some 500,000–1,000,000 SNPs [8,9]. Although this type of approach has a number of known issues, *e.g.*, its extreme cost, limited statistical power or that it explains only a small percentage of phenotypic variance [4,10], these studies provide the scientific community with the ability to work without prior hypotheses. In general, they all point to a few biological pathways: Wnt/β-catenin signaling, estrogen endocrine, RANKL/RANK/OPG, bone ossification, mesenchymal-stem-cell differentiation, osteoclast differentiation and the TGF-signaling pathways [8,9,11–13]. Nevertheless, there about 30 BMD GWAS loci which lack prior molecular or biological evidence of involvement [12]. Finally, another approach consists of trying to define the mechanisms that underlie the association with phenotype performance, for example, animal models in which the gene has been mutated, over-expressed or deleted [10].

In this paper, we have analyzed the global gene expression through microarrays in bone marrow of OVX mice and compared it with that of SHAM operated control mice to identify genes showing differential expression in response to the estrogen deficiency induced by OVX. We decided to study bone marrow since it is in the microenvironment of this tissue where the main cells involved in bone homeostasis are located and because it represents a direct target of the effect of estrogen depletion. With this approach, we have tried to reproduce one of the major risk factors for osteoporosis in women, the estrogen deficiency that occurs at menopause or after a bilateral ovariectomy [14]. To our knowledge, we are the first to develop this translational research approach for studying the genetics of postmenopausal osteoporosis. The method consists of first identifying differentially expressed genes in response to OVX in an experimental animal model, and second, studying the association of some human genes orthologous to those differentially expressed in mice with BMD, in a cohort of women in order to establish whether they are susceptibility genes to postmenopausal osteoporosis.

Materials and methods

Mice and treatments

Fifteen-week-old, skeletally mature female C57BL/6 mice (Charles River Laboratories, Barcelona, Spain) were housed in an environmentally controlled laboratory upon arrival and acclimatized for 3 days. After this period, the animals were either dorsal ovariectomized (OVX, N = 23) or sham operated (SHAM, N = 14) under general anesthesia using 0.1 mg/kg Butorphanol (Torbugesic, Fort Dodge Laboratories, Girona, Spain) as a pre-anesthetic, 5% isoflurane to induce anesthesia and 1.5% isoflurane as maintenance (Veterinaria Esteve, Barcelona, Spain), and maintained as previously described [15]. One mouse from the SHAM group died as a consequence of the intervention. None of the other mice exhibited evidence of infectious disease, impaired growth, immunosuppression, or other side effects.

Four weeks after surgery the mice were sacrificed to obtain the right femur, having assessed the success of ovariectomy, as previously described [15]. One mouse of the OVX group was discarded because it did not show the expected uterine atrophy. The bone marrow cells were isolated from the femora of animals using centrifugation [16] then lysed immediately with 1 mL TRIzol (Invitrogen, Carlsbad, CA). All procedures for consideration of animal welfare were reviewed and approved by the ethical committee of our institution.

RNA isolation and GeneChip expression analysis

Total RNA from bone marrow cells was extracted using the TRIzol reagent and was purified using the PureLink Total RNA Purification System (Invitrogen) following the manufacturer's instructions. All RNA samples inside the purification column were treated with RNase-Free DNase for removal of contaminating DNA (Invitrogen). Purified total RNA was stored at −80 °C until used as a template for cDNA synthesis. RNA integrity was assayed by means of the 2100 Bioanalyzer (Agilent Technologies, Santa Clara, CA, USA) and RNA concentration was determined by measuring absorbance at 260 nm using a highly sensitive capillary spectrophotometer (GeneQuant, GE Healthcare Biosciences). Equal amounts of purified RNA extracted from 13 SHAM-operated mice and from 22 OVX mice were pooled in three (SHAM) and in five (OVX) pools, with each containing 4–5 different RNAs from individual mice. The generation of mRNA pools is a standard method to reduce the effect of biological replication [17]. Consequently, a total of 8 microarrays were developed and analyzed in the present study: three for SHAM mice (named C1–C3) and five for OVX mice (named O1–O5).

The synthesis of cDNA and cRNA, labeling, hybridization and scanning of the samples were performed as described by the GeneChip Expression Analysis Technical Manual (Affymetrix Ltd., UK), as previously described [18]. Twenty micrograms of fragmented biotinylated cRNA were used to prepare the hybridization cocktail and subsequently hybridized for 16 h at 45 °C for the Affymetrix GeneChip Mouse Expression Array 430 2.0, which contains of 45,101 probe sets, representing over 14,000 well-characterized genes. Arrays were washed, scanned and analyzed to obtain CEL files from pixel values on the DAT files, as previously described [18]. Global differences between different samples (CEL files) were measured by principal component analysis (PCA), linear discriminant analysis (LDA), and hierarchical clustering using the Partek Genomic Suite software (Agilent). For hierarchical clustering analysis, Pearson's dissimilarity was used to calculate row dissimilarity, and Ward's method was used for row clustering.

The analysis of significant changes in expression profiles of SHAM *vs.* OVX mice was done by GEPAS 4, a web-based tool (http://www.gepas.org) [19]. Briefly, for global background subtraction and cross array normalization, we used the Robust Multichip Average (RMA) method; for between array standardization methods, we used the quantiles tool, and for PM–MM adjustment we used the PM-only tool, and only PM values were taken into account [19]. The probe-set summary method was performed by using the median polish tool, which uses Tukey's median polish procedure to compute probe-set summaries. T-Rex was the tool used for analyzing differential gene expressions. It implements several modules to study gene expression under different experimental conditions. For each gene, this tool performs a t-test for the difference in mean expression between the two groups of arrays (SHAM and OVX), and T-statistics and *P*-values are reported. In the present work, significant genes from the comparison between SHAM and OVX mice were selected using the Benjamini–Hochberg method to control for a maximum false discovery rate (FDR) in the multivariate system. Only adjusted *P*-values <0.001 and a FDR used to discriminate false positives in the multivariate system <0.15 were considered as significantly different between groups.

The genes differentially expressed in response to OVX were visualized in biological pathways with the Ingenuity Pathways Analysis mapping software (IPA; Ingenuity Systems, Redwood City, CA; www.ingenuity.com). Data sets containing the Affymetrix probe set identifiers and T-statistics obtained from the t-test for the difference in mean expression between the two groups of arrays were uploaded to the application. In

our experiment a set of 180 genes identifiers of transcripts, which displayed a significant change in response to OVX as compared to control SHAM operated mice (FDR < 0.15; $P < 0.0007$), were uploaded and analyzed, as previously described [18].

MassARRAY quantitative gene expression (QGE)

In order to validate the differential expression found in the microarray experiment, we performed real competitive PCR and Matrix Assisted Laser Desorption/Ionization Time-of-Flight (MALDI-TOF) mass spectrometry (Sequenom, CA, USA) analysis using 4 replicates of each of the 12 different RNAs from each group of mice (SHAM or OVX) for 12 selected genes with 8 dilutions of competitor in each experiment. Likewise, a set of 4 housekeeping genes (*Gadph*, *Actb*, *Hprt1*, and *Tubb5*) were used as endogenous controls for gene expression normalization. For each gene, a 70–120 bp region of identical sequence with one single mismatch was chosen according to the analysis performed by the software. One microgram of total purified RNA was reverse transcribed into cDNA using the ThermoScript RT-PCR System (Invitrogen), following the manufacturer's instructions, with a mix of random hexamers and oligo(dT). Then, cDNA was diluted 1/10 in water, and 1 μL of this dilution, along with the synthetic competitor having the single mismatch, served as templates for competitive PCR. All PCR primers and competitors were designed using the Multiplexed QGE Assay Design 3.4 software (Sequenom; Supplemental Table S1). The removal of excess dNTP, the primer extension reaction, and the RNA quantification were performed as described in the Sequenom application guide (http://www.sequenom.com).

Subjects

The study group we analyzed to assess the associations of SNPs with bone density in specific, differentially expressed genes obtained from the animal OVX model consisted of a postmenopausal female population of Spanish ancestry living in Valencia that are part of a cohort that we have regularly utilized in genetic association studies [20–22]. A total of 706 women with natural menopause, defined by at least 1 year of amenorrhea and follicle-stimulating hormone (FSH) level above 40 UI/mL, or subjected to a bilateral ovariectomy performed before menopause, consented to participate in the study and underwent genotyping. At the hospital, on the day of blood extraction to obtain DNA and/or serum, each woman received a questionnaire about osteoporosis risk factors, *e.g.*, age, height and weight, cigarette smoking and use of hormone therapy (HT) or medications known to affect bone metabolism, and the data were recorded.

Women with a history of bone disease other than primary osteoporosis or who had used any medication known to alter bone mass, except for HT, were excluded from the study. Age, years since menopause (ysm), weight, smoking, and HT-use were used as covariates in the analysis of the data. The local ethics committee approved the study and protocol, and written informed consent was obtained from all women in accordance with the regulations of the INCLIVA Institute of Health Research and the Ethics Committee of our center.

Anthropometric and bone mineral density (BMD) data

The BMI was calculated for each participant as the ratio between weight (kg) and height squared (m^2).

In the present study, almost all of the women underwent a densitometric study at femoral neck (FN) and at lumbar spine (LS) sites by dual energy X-ray absorptiometry (DXA) at the non-dominant proximal FN (FN-BMD; N = 626) and at the LS from L2–L4 (LS-BMD; N = 638). We used a Norland XR-36 (Norland Medical Systems Inc.; Fort Atkinson, WI, USA) or Lunar DPX (GE Lunar Corporation, Madison, WI, USA) densitometers. In order to manage BMD performed with two different densitometers, a standardized BMD (sBMD) was calculated [21,22], and "type of densitometer" was used as a covariate in the multivariate analysis.

Single nucleotide polymorphisms (SNPs) and genotyping

In the present work, we decided to analyze the association of BMD in our cohort of women for polymorphisms belonging to 4 genes that showed differential expression after OVX in mice. Two genes, the serum glutathione peroxidase 3 gene (*GPX3*, plasma) and the interleukin-1 receptor-associated kinase 3 gene (*IRAK3*), showed a decreased expression in the bone marrow of the OVX mice, while the other two genes, the molecule immunoglobulin-associated alpha gene (*CD79A*) and the interleukin 7 receptor gene (*IL7R*), showed an increased expression after OVX. The genes were chosen because all except the *CD79A* gene have been previously associated with bone loss. That notwithstanding, none of these genes have been studied for an association with BMD in humans to date [23–25].

The dbSNP database of the National Center for Biotechnology Information (NCBI) was explored to identify SNPs of the *GPX3*, *IRAK3*, *CD79A* and *IL7R* genes in the Caucasian population. Then, haplotype blocks were constructed with Haploview 4.2 software (http://www.broad.mit.edu/mpg/haploview/) using the Gabriel method [26]. SNPs were selected in different haplotype blocks looking for SNPs with adequate heterozygosity and with a minor allele frequency in Caucasians of >5% with the use of FastSNP (http://fastsnp.ibms.sinica.edu.tw/), a web-based tool, to identify potentially functional SNPs in the genes.

Thus, for the *IL7R* gene (chromosome 5), the Haploview software detected a single haplotype block of 33 kb, and we selected three SNPs: rs6897932 (C>T, chromosome position, 35874575, Build 37), rs11567705 (C>G, 35861152) and rs2228141 (C>G, 35871273). For the *CD79A* gene (chromosome 19), the software showed no clear haplotype blocks, probably due to the low number of SNPs characterized in this region with adequate heterozygosity. We selected two SNPs in this gene: the rs3810153 (A>G, 42385469) and rs1428922 (G>A, 42379780). For the *GPX3* gene (chromosome 5), the software detected three haplotype blocks of 2 kb, 5 kb and less than 1 kb. We selected three SNPs belonging to the first two blocks: rs1946234 (A>C, 150399210), rs3792796 (G>C, 150402490), and rs8177447 (T>C, 150407456). Finally, for the *IRAK3* gene (chromosome 12), the analysis showed two haplotype blocks of 51 kb and 1 kb. We selected 6 SNPs in the larger block and one in the smaller one: rs1732887 (G>A, 66581616), rs1168771 (T>C, 66588836), rs1168760 (A>T, 66595850), rs2289134 (T>C, 66598687), rs1152888 (A>G, 66605228), rs1623665 (T>G, 66618182), and rs1152916 (A>T, 66635304). The analysis with FastSNP software showed a medium-high risk for rs1152888 SNP (*IRAK3*) because it could affect splicing sites, and a low-medium risk for rs6897932 and rs2228141 (*IL7R* gene) SNPs because they could affect splicing regulatory sites. For the remaining SNPs, the FastSNP software assigned a low risk of affecting gene expression.

Obtaining DNA from blood samples and genotyping SNPs by allelic discrimination using TaqMan® SNP Genotyping Assays (Applied Biosystems, Foster City, CA) on a 7900 HT Fast Real-Time PCR System (Applied Biosystems) were performed as previously described [22]. The reproducibility of the technique was approximately 100% and was estimated in each PCR by re-genotyping about 7–8% of the samples in each plate. In about 0–4% of the samples, we were unable to get a valid genotype. This was because of a poor amplification mainly as a result of the concentration or quality of the DNA. All these samples were re-genotyped by changing some of the protocol parameters: by increasing the amount of DNA in the PCR, by reducing the annealing temperature or by increasing the number of PCR cycles.

Statistical analysis

Beginning with the mouse experiments, we used the statistical tools included in the GEPAS 4 software. A t-test was used to detect differences in mean expression between the two groups of arrays (SHAM and OVX), reporting t-statistics and *P*-values. To control for a maximum false discovery rate (FDR) in the multivariate system, we used the Benjamini–Hochberg method and only adjusted *P*-values <0.0007 and

an FDR <0.15 were considered as significantly different between groups.

Then, to test the homogeneity of the participant women, genotypic frequencies for each polymorphism were tested against Hardy–Weinberg Equilibrium (HWE) proportions by standard χ^2 tests and with the use of SNPStats software (http://bioinfo.iconcologia.net/index.php?module=Snpstats) [27]. In addition, the presence of population stratification was evaluated with STRUCTURE software, running a dataset with five markers belonging to different chromosomes [28]. The model of inheritance (co-dominant, dominant, over-dominant and recessive) was analyzed with SNPStats. The significance threshold after a multiple test correction for each gene was estimated by considering the effective number of independent marker loci, using the single nucleotide spectral decomposition software (SNPSpD) developed by Nyholt [29].

Fixed-effects designs of analysis of variance (ANOVA) were used for comparisons of means between groups. Analysis of covariance (ANCOVA) and regression analysis were used to examine differences in BMD and in age-adjusted BMD (Z-score) according to genotype, after adjustment for confounder variables like age, ysm, weight, HT use (nonuser, user), smoking status (nonuser-user), and type of densitometer. ANCOVA analyses were corrected for multiple testing by Bonferroni's correction method (SPSS software). Automated binomial logistic regression analysis with forward stepwise variable selection was used to estimate the relative risk of osteopenia or osteoporosis according to the WHO definition (T-score ≤ -1). In each analysis, odds ratios (with 95% confidence intervals) adjusted by the above-mentioned confounder variables were calculated.

We estimated sample size of 686 as sufficient to get an 85% statistical power. This was done in order to detect a gene effect of $R^2 = 0.013$ (estimated by regression analysis between LS-BMD and rs148922 SNP) according to a frequency for the A allele of 0.49 (Table 1) under a recessive model of inheritance and a mean ± SD for LS-BMD of 0.993 ± 0.151 g/cm^2 for the entire population (Table 2). We used the QUANTO software package (http://hydra.usc.edu/GxE/) [30] for this.

Values shown in the text, tables and figures are means ± SD and frequencies, unless otherwise specified. All analyses were two-tailed, and significance was defined as $P < 0.05$, except when multiple comparisons were analyzed. The statistical analysis was carried out using the Statistical Package for Social Sciences (version 19; SPSS Inc., Chicago, IL).

Table 1
Genotypic and allele frequencies and HWE *P*-values for the polymorphisms analyzed.

Gene	SNP	Genotype	N (frequency)	Allele (frequency)	HWE *P*-value
GPX3	rs1946234	A/A	571 (0.81)	A (0.90)	1.00
		A/C	127 (0.18)	C (0.10)	
		C/C	7 (0.01)		
	rs3792796	C/C	271 (0.39)	C (0.61)	0.20
		C/G	315 (0.45)	G (0.39)	
		G/G	112 (0.16)		
	rs8177447	C/C	429 (0.61)	C (0.78)	0.91
		C/T	244 (0.35)	T (0.22)	
		T/T	33 (0.05)		
IL7R	rs6897932	C/C	410 (0.58)	C (0.76)	0.35
		C/T	247 (0.35)	T (0.24)	
		T/T	45 (0.06)		
	rs11567705	C/C	408 (0.58)	C (0.76)	0.41
		C/G	247 (0.35)	G (0.24)	
		G/G	44 (0.07)		
	rs2228141	C/C	483 (0.69)	C (0.83)	0.89
		C/T	200 (0.28)	T (0.17)	
		T/T	19 (0.03)		
CD79A	rs3810153	A/A	240 (0.35)	A (0.59)	1.00
		A/G	331 (0.48)	G (0.41)	
		G/G	114 (0.17)		
	rs1428922	A/A	164 (0.23)	A (0.49)	0.29
		A/G	365 (0.52)	G (0.51)	
		G/G	172 (0.25)		
IRAK3	rs1732887	T/T	356 (0.51)	T (0.71)	0.41
		T/C	280 (0.40)	C (0.29)	
		C/C	64 (0.09)		
	rs1168771	C/C	129 (0.19)	C (0.41)	0.028
		C/T	306 (0.44)	T (0.59)	
		T/T	257 (0.37)		
	rs1168760	A/A	616 (0.89)	A (0.94)	0.72
		A/T	78 (0.11)	T (0.06)	
		T/T	1 (0.00)		
	rs2289134	T/T	326 (0.47)	T (0.68)	0.082
		T/C	282 (0.41)	C (0.32)	
		C/C	83 (0.12)		
	rs1152888	A/A	1 (0.00)	A (0.06)	0.72
		A/G	78 (0.11)	G (0.94)	
		G/G	622 (0.89)		
	rs1623665	G/G	280 (0.40)	G (0.62)	0.025
		G/T	300 (0.43)	T (0.38)	
		T/T	115 (0.17)		
	rs1152916	A/A	193 (0.28)	A (0.53)	1.00
		A/T	348 (0.50)	T (0.47)	
		T/T	155 (0.22)		

Results

Microarray and gene expression profile analysis of differentially expressed genes after OVX

To detect and quantify the differential gene expression induced by OVX, we used the T-Rex software (GEPAS suite) which, for each gene, performed a t-test for the difference in mean expression between the two groups of arrays. Subsequently, the analysis showed 180 significant transcripts (Supplemental Table S2), of which 120 genes were up-regulated (66.7%) and 60 genes (33.3%), were down-regulated. The sign of the T-statistics (Supplemental Table S2) indicates whether a given gene expression was up-regulated with OVX (plus sign) or down-regulated (minus sign).

Principal component analysis (PCA) was applied to detect the interrelationships among the pools of samples used in the present study. PCA is an exploratory technique used to define the structure of high-dimensional data (*e.g.*, microarray data) by reducing its dimensionality. The analysis of the projections of these components on spatial axes provides insight into the different patterns of gene expression in each group of samples. Fig. 1 shows the PCA for the eight experimental pools (5 pools for OVX mice and 3 pools for SHAM mice), and the mean for each group. It is clear that both groups are adequately separated into two sets, showing that the gene expression profiles in the mRNA pools of both groups are essentially different, although the samples from the OVX group showed greater dispersion than did those from the SHAM controls. Hierarchical clustering collects similar entities into clusters, producing a dendrogram that shows the hierarchy of the clusters. In the present work, it was also used to analyze the expression

Table 2
Anthropometric and bone characteristics of the Spanish postmenopausal female cohort studied (mean ± SD or percentage).

	Number	Values
Age (year)	706	53.2 ± 6.6
Years since menopause (year)	706	6.2 ± 5.6
Weight (kg)	706	66.3 ± 11.3
Height (cm)	706	157.3 ± 6.2
BMI (kg/m^2)	706	26.8 ± 4.4
Smoking (%)	706	24.5
HT user (%)	706	34.6
Surgical menopause (%)	706	28.0
FN-BMD (g/cm^2)	626	0.799 ± 0.122
FN T-score	626	−0.93 ± 1.05
FN Z-score	626	−0.09 ± 1.01
LS-BMD (g/cm^2)	638	0.993 ± 0.151
LS T-score	638	−1.16 ± 1.41
LS Z-score	638	−0.24 ± 1.25

BMI, body mass index; HT, hormone therapy; BMD, bone mineral density; FN, femoral neck; and LS, lumbar spine.

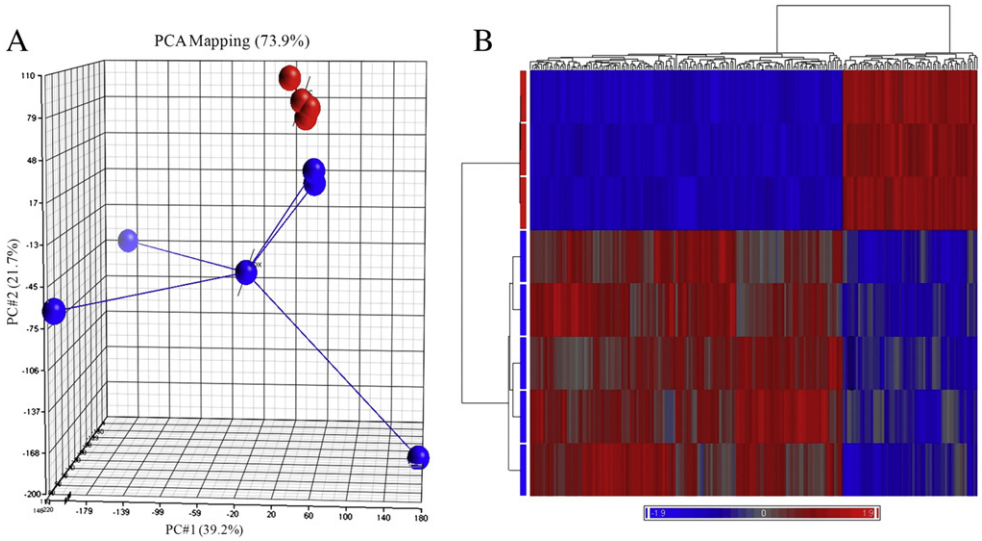

Fig. 1. A) Principal components analysis (PCA) and B) hierarchical clustering of transcriptome data from SHAM (red) and OVX (blue) mice.

profile between OVX and SHAM samples (Fig. 1). The results show that there is broad agreement on gene expression profiles among arrays hybridized with mRNA from SHAM mice and among arrays hybridized with mRNA from OVX mice. This result would be consistent with the image provided by the PCA analysis and, although there is some scatter in the pools of OVX mice, the gene expressions for both samples can be easily clustered.

Identification and functional classification of differentially expressed genes induced by OVX

In order to classify the OVX-induced genes in terms of their biological function, IPA software was used. This classification showed that OVX altered the expression of genes involved in biological functions like skeletal and muscular diseases (62 genes), connective tissue diseases (45 genes), immunological diseases (49 genes), proliferation and cell growth (49 genes), function and development of the hematological system (35 genes), or those related to humoral immune response (22 genes), among others. The top five canonical pathways, based on their significance (*P*-value), included B-cell development ($P = 1.3 \times 10^{-7}$), primary immunodeficiency signaling ($P = 2.9 \times 10^{-6}$), PI3K signaling in B lymphocytes ($P = 5.7 \times 10^{-5}$), phospholipase C signaling ($P = 6.1 \times 10^{-5}$), and FcgRIIB signaling in B lymphocytes ($P = 7.3 \times 10^{-4}$).

The IPA analysis showed 23 significant regulatory networks (score > 2), of which the 10 most significant (score > 12) are displayed in Supplemental Table S3. The number one ranked network (score =

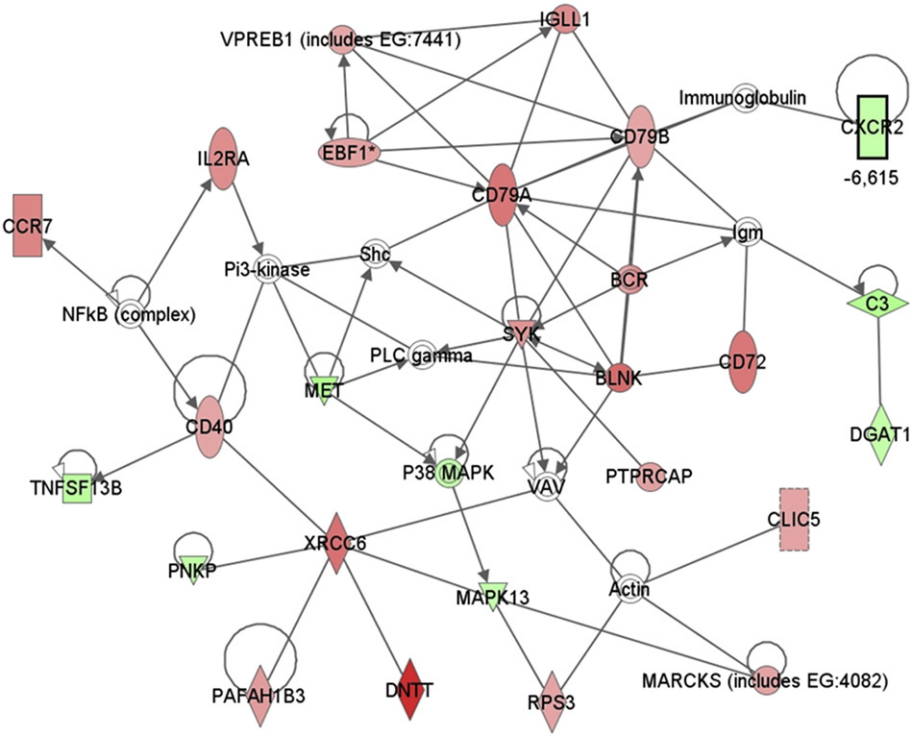

Fig. 2. The most significant network regulated by OVX in mice bone marrow. The intensity of the node color indicates the degree of up- (red) or down- (green) regulation. Only direct relationships between genes are represented.

43, focus genes = 25) (Fig. 2) is associated with cellular development, hematological system development and function, and humoral immune response. This network is focused on genes like the BCR (B-cell receptor) and its members CD79A and CD79B (immunoglobulin-associated alpha and beta antigens), BLNK (B-cell linker), SYK (spleen tyrosine kinase), and CD40 gene (TNF receptor superfamily member 5). All these genes participate in processes such as B-cell activation, B-cell differentiation, B-cell proliferation, B-cell receptor signaling pathway, humoral immune and inflammatory response, intracellular signal transduction pathways, and the positive regulation of bone resorption, among many others. Top functions of some other highly significant networks are associated with skeletal and muscular disorders (e.g., *Galnt3*, *Ebf1*, *Ibsp*, *Gata1*, *Sox4*, or *Gh* genes), phospholipase C signaling, PI3K signaling in B lymphocytes, cell death, endocrine system disorders, lipid metabolism, cellular assembly and organization cell signaling, and hematological disease, among others (Supplemental Table S3).

Microarray analysis validation by MassARRAY QGE analysis

To validate the results obtained by the gene expression with microarray analysis, a MassARRAY QGE analysis was performed using the same RNA samples analyzed in the microarray experiment for 12 selected genes. In this case, though, the samples were analyzed individually instead of by pools (Table 3). For eight of the twelve genes examined using this technique, we detected significant differences between SHAM and OVX mice, indicating that the results of the microarray study provided reliable comparisons between both groups of mice. The significant differences were not 100%, probably due to dispersion in the molar concentration of RNA for some genes whose value ranged from 10^{-16} to 10^{-22} M.

Association studies of differentially expressed genes in the cohort of women

The main objective of this study was to find genes whose expression changes in response to OVX in order to analyze the association of these genes with bone phenotypes in our cohort of postmenopausal women using a translational approach. Consequently, we decided to study, in our cohort of women, the association of BMD with two genes that showed a lower expression in OVX mice (*GPX3* and *IRAK3*) and with two genes that showed an increased expression in OVX mice (*CD79A* and *IL7R*). Supplemental Fig. S1 shows the fluorescence intensity values for each pool of samples (blue: OVX; red: SHAM) showing that with OVX, gene expressions for *Irak3* and *Gpx3* were down-regulated, whereas the expressions for *Il7r* and *CD79a* were up-regulated.

Table 3
Validation of microarray results by MassARRAY QGE analysis (Sequenom). The T-statistics is the value obtained from the analysis of differential gene expression by T-Rex software (GEPAS suite). The ratio OVX/SHAM results from dividing the molar concentration of each gene in bone marrow between OVX mice (12 animals) and SHAM mice (12 animals) obtained with Sequenom. The PCR and competitor primers are shown in Supplemental Table S1.

Gene	T-statistics (GEPAS)	Ratio OVX/SHAM (Sequenom)	*P*-value (Sequenom)
Dntt	17.4	2.20	0.170
Sox4	12.7	2.35	0.099
Il7r	12.4	2.61	0.037
Dpp4	12.3	2.56	0.000058
Blnk	11.3	3.52	0.00027
CD79a	10.3	2.59	0.000025
CD72	10.2	2.31	0.002
Capsl	9.5	2.35	0.015
Cpm	8.2	2.88	0.00015
Tnfrsf19	6.9	2.08	0.148
CD40	6.5	1.82	0.320
Gpx3	−7.8	0.39	0.004

The main characteristics of the 706 participants in the study are listed in Table 2. Note that women displayed normal bone parameters according to their median age, showing a mild osteopenia at the lumbar spine site (T = −1.16 ± 1.41). Genotype, allele frequencies and the Hardy–Weinberg Equilibrium (HWE) *P*-values for the SNPs examined in the present study are shown in Table 1. The genotyping rate for the 15 SNPs analyzed was higher than 99%. The allelic frequencies were similar to those reported in other Caucasian populations, and the distribution frequencies for 13 of the 15 SNPs were consistent with the HWE. Two SNPs showed departures from HWE with nominal *P*-values <0.05 (0.028 and 0.025, respectively for the *IRAK3* gene). However, both were above the threshold significance of 0.009 after multiple test correction (Table 1). An analysis with STRUCTURE software showed data consistent with a single population ($P > 0.99$), while models assuming two-to-five populations revealed negligible probabilities, which is incompatible with the existence of substructures or stratification in our population.

A preliminary study, by means of ANOVA (not shown), detected significant and/or suggestive associations of SNP rs8177447 in the *GPX3* gene with the femoral neck (FN)-BMD ($P = 0.114$) and of SNPs rs3810153 and rs1428922 in the *CD79A* gene with the lumbar spine (LS)-BMD ($P = 0.077$ and $P = 0.018$, respectively). The SNPStats software assigned a dominant model of inheritance to rs8177447 (dominant allele T, $P = 0.048$) in the *GPX3* gene and recessive models of inheritance for both rs3810153 (recessive allele G, $P = 0.047$) and rs1428922 (recessive allele A, $P = 0.009$) in the *CD79A* gene. Consequently, women of the CT and TT genotypes for rs8177447 SNP, of the AA and AG genotypes for rs3810153 SNP and of the GG and GA genotypes for rs1428922 SNP were combined. Table 4 shows the FN and LS BMD and Z-scores according to these combinations, adjusted for the covariates age, ysm, weight, smoking, HT-user and densitometer type. Women with the CC genotype for rs8177447 showed significant bone deterioration at the FN site, although the same trend was also observed for the LS. Similarly, homozygous women for the G allele of rs3810153 and for allele A of rs1428922 showed lower bone parameters at the LS site than did the other women, with very clear bone deterioration for the latter SNP ($P = 0.001$ and $P = 0.002$ for the LS-BMD and LS-Z-score, respectively).

Finally, we conducted a multiple regression model, adjusting for age, ysm, BMI, densitometer type, HT use and smoking status, to evaluate the risk of FN and LS osteopenia or osteoporosis (Table 5). In this study, we selected women with osteopenia or osteoporosis because, in our population, less than 4.9% of women have FN osteoporosis (T < −2.5). For FN, the odds ratio for osteopenia or osteoporosis for women of the CC genotype for rs8177447 compared with CT/TT women was slightly higher (OR: 1.5, $P = 0.014$), but the risk for osteopenia or osteoporosis for women GG and AA for rs3810153 and rs1428922, respectively, was significantly higher (OR: 1.8 and 1.7, respectively).

Discussion

Antecedents and main purpose of the present study

In recent years dozens of GWAS have been carried out in order to identify genes involved in complex diseases. These studies, on the one hand, are increasing the number of genes associated with phenotypes of interest, often detecting unexpected pathways and genes. On the other hand, they are concluding that, among all the genes associated with a phenotype, we can explain only a small part of the total phenotypic variance of that phenotype. This, at least in part, may be a result of the huge imposition on the statistical treatment caused by the issue of multiple comparisons. It may also be revealing that the methodological approach which uses common variants for association analysis has reached its limit, and that other approaches need to be considered. Some of these alternatives to find the missing heritability could be the study of rare variants, the management of functional tests for the search

Table 4
FN- and LS-BMD and Z-scores adjusted by age, ysm, weight, smoking, HT-user and densitometer type in our population according to rs8177447 (*GPX3*), rs3810153 (*CD79A*) and rs1428922 (*CD79A*) SNP genotypes. Values are mean ± SEM. The *P*-value is the value calculated by the statistical software after applying the Bonferroni correction for multiple comparisons.

Locus	Femoral neck		Lumbar spine	
	BMD (g/cm^2)	Z-score	BMD (g/cm^2)	Z-score
rs8177447 (*GPX3*)				
CC	0.793 ± 0.006	−0.16 ± 0.05	0.990 ± 0.007	−0.29 ± 0.06
CT/TT	0.813 ± 0.008	0.02 ± 0.07	1.002 ± 0.009	−0.16 ± 0.08
P-value	0.043	0.031	0.331	0.202
rs3810153 (*CD79A*)				
AA/AG	0.805 ± 0.005	−0.06 ± 0.04	1.001 ± 0.006	−0.19 ± 0.05
GG	0.786 ± 0.011	−0.23 ± 0.10	0.964 ± 0.014	−0.48 ± 0.12
P-value	0.134	0.107	0.016	0.024
rs1428922 (*CD79A*)				
GG/GA	0.805 ± 0.005	−0.06 ± 0.05	1.005 ± 0.007	−0.16 ± 0.06
AA	0.789 ± 0.010	−0.20 ± 0.09	0.959 ± 0.012	−0.52 ± 0.10
P-value	0.168	0.139	0.001	0.002

and identification of candidate genes or the analysis of underlying epigenetic mechanisms [31].

The present study represents an example of translational research that aims to identify genes associated with osteoporosis using one of these alternative methodologies. Indeed, we have analyzed the changes in global gene expression induced by OVX in mouse bone marrow in order to identify potential candidate genes to translate the study to our cohort of women. The reasons for choosing this animal model have been the knowledge that estrogen deficiency is the primary cause of osteoporosis in women [14], the fact that mice subjected to OVX is widely accepted as a valid approach to study this deficit, and because our group already had previous experience with this model [15,32,33].

Genes and pathways altered in mouse bone marrow after ovariectomy

We have detected 180 genes whose expression changed due to the OVX, most of them experiencing an up-regulation, as previously described [34]. In order to confirm the validity of the microarray experiment, we have used MassARRAY QGE (Sequenom) analysis, and we obtained statistical significance in eight of the twelve genes analyzed. For the other four genes, there was a trend among the microarray and Sequenom results, as the OVX/SHAM ratios and *P*-values show (Table 3). We consider that there are two main reasons for this non-absolute correlation. The first one is that in the Sequenom study, individual mRNAs were used instead of pools. The second one is that for some transcripts, molar concentration was very low and therefore, highly variable, which makes it more difficult to reach statistical significance when using individual mRNAs.

Canonical pathway analysis revealed the B-cell differentiation, development and activation as the most significant signaling pathways in bone marrow of mice one month after OVX (Supplemental Table S3 and Fig. 2). Among the genes whose expression was changed with the OVX in this most significant signaling pathway, there are genes involved in B-cell signal transduction (*Bcr*, *Blnk*, *CD79a*, *CD79b*, *Syk*), in B-cell differentiation (*Vpreb1*, *Igll1*, *Ebf1*, *Syk*, *Dntt*) and in B- and T-cell activation (*Ptprcap*, *Tnfsf13b*, *Mapk13*, *Il2ra*, *CD40*, *Ccr7*). It is well-known that estrogen deficiency induces B-lymphopoiesis [33,35], a process that could be implicated in bone loss associated with this deficiency, although the participation of B-cells in bone loss is controversial. For example, it has been reported that the administration of IL7 to the mouse induces B-lymphopoiesis and osteoclastic bone destruction [36], that mature B-cells and their precursors can express RANKL [37], that B-cell precursors have the capacity to differentiate directly into bone resorbing osteoclasts [38], and that the depletion of B-cells in patients with rheumatoid arthritis suppresses bone turnover [39]. To the contrary, it has been reported that ovariectomy-induced bone loss occurs independently of B-cells [40], that B-cells are the main producers of the anti-osteoclastogenic factor OPG, that B-cell knockout mice are osteoporotic [41], and that mature peripheral blood B-cells inhibit osteoclast formation in an *in vitro* model of human osteoclastogenesis by a mechanism involving TGF-β [42]. Despite this controversy, it is accepted that activated B-cells may be potent regulators of bone resorption [43]. In fact, the *IL2ra* (CD25) gene, which is a marker of cell activation, is up-regulated in the present study and as previously described [32,33], indicating that OVX induces activation of B- and T-cells [44].

Table 5
Estimation of risk for FN and LS osteopenia or osteoporosis, adjusted by age, ysm, weight, smoking, HT-user and densitometer type, according to genotypes that were associated with BMD.

Site	Genotype	*P*-value	Odds ratio	95% CI
Femoral neck	CC *vs.* CT/TT (rs8177447)	0.014	1.548	1.090–2.196
Lumbar spine	GG *vs.* AA/AG (rs3810153)	0.012	1.816	1.139–2.894
	AA *vs.* GG/GA (rs1428922)	0.013	1.706	1.121–2.597

Previous associations with bone metabolism of some genes altered after ovariectomy

Whatever the role of B-cells in the regulation of bone homeostasis, in the most significant canonical pathway there are genes which have been previously associated with bone metabolism (Supplemental Table S3). Thus, for example, *Syk* and *Blnk* genes (both up-regulated by OVX) intervene in the regulation of osteoclast differentiation by linking RANK and ITAM signals [45], the *in vivo Fbf1* (up-regulated) overexpression in osteoblasts results in suppressed bone formation [46], and the *Marcks* gene (up-regulated) is necessary for the regulation of bone resorption through protein kinase C-delta (PKCδ) [47]. The behavior (up- or down-regulation) that these genes have shown in the bone marrow of ovariectomized mice would be consistent with the increased bone loss established after OVX. Other genes not included in this most significant canonical pathway have also been previously associated with bone phenotypes. Thus, for example, *Ibsp* (down-regulated), *Galnt3* (down-regulated) and *Sox4* (up-regulated) genes were found to be associated with bone phenotypes in a recent GWAS with replication in two independent datasets [48]. Similarly, *Foxp1* (up-regulated), *Plcb1* (down-regulated), *Dpp4* (up-regulated), *Sox5* (up-regulated), *Mapk13* (down-regulated) and *Clic5* (up-regulated), among others, have been reported to regulate the activity of cells involved in bone homeostasis, in fracture healing and in bone loss in certain circumstances like OVX [49–54]. Of interest is the increase in CD40 expression induced by OVX. Our group has previously described the association of polymorphisms in CD40 and CD40L genes with bone mass and osteoporosis risk [22,55]. The system formed by CD40/CD40L is essential to the

immune response but also seems to be so to bone metabolism. In fact, CD40- and CD40L-deficient mice have an osteopenia similar to that of children with Hyper-IgM syndrome as a result of mutations in the CD40L gene [41,56]. The mechanism by which the CD40/CD40L system intervenes in bone metabolism is not fully elucidated. It is known, for example, that signaling through CD40 induces the expression of OPG by B-cells, but it has also been described that when T-cells are activated, as is the case in the OVX or in the continuous administration of PTH, signaling through CD40 expressed in osteoblasts or mesenchymal cells induce pro-osteoclastogenic signals and bone loss [41,44,57].

Translating the results achieved in the animal model to our cohort of women

After the analysis of global gene expression in the mouse, we selected four genes for further study, analyzing their association with BMD in our cohort of postmenopausal women. The main criterion for this selection, based on our present knowledge, was that gene function has a potential physiological relevance to bone function. With this premise, two down-regulated genes (*GPX3*, serum glutathione peroxidase 3; and *IRAK3*, interleukin-1 receptor-associated kinase 3) and two up-regulated genes (*CD79A*, immunoglobulin-associated alpha gene; and *IL7R*, interleukin 7 receptor), were selected. All of the genes except the *CD79A* gene have been previously associated with bone metabolism [23–25], although none of these genes has been studied in epidemiological studies of osteoporosis. *CD79A* was selected because it seems to have an important role in the most significant canonical network (Fig. 2).

Two of the studied genes in this translational approach were significant in our cohort of women (Tables 4 and 5). The *GPX3* gene codifies for the serum glutathione peroxidase 3, an enzyme that is decreased in aged osteoporotic female rats [25] and in mice subjected to OVX (the present study). This enzyme intervenes in the detoxification of hydrogen peroxide so it is an important barrier against reactive oxygen species (ROS) and their consequences for cell function. Indeed, it is well-known that ROS may contribute to aging and osteoporosis resulting from marked decreases in plasma antioxidants in aged women and men, and that the loss of estrogens or androgens diminishes defenses against oxidative stress in bone. This explains, in part, increased bone resorption when this hypogonadism arises [58]. Consequently, the decrease of *GPX3* in bone marrow of OVX mice observed in the present study supports the involvement of this enzyme in bone loss due to estrogen deficiency and reinforces the importance of ROS in bone homeostasis. Regardless of this, the SNPStats software assigned a low risk to the SNPs of this gene, so it is not likely to be a functional polymorphism. Rather, it may be in linkage disequilibrium with other variants of the *GPX3* gene or other causative genes near the region, like *TNIP1* (TNFAIP3 interacting protein 1) which has been associated with pathologies such as rheumatoid arthritis.

The other gene associated with bone phenotypes in our cohort of women was *CD79A* (Ig-alpha, immunoglobulin-associated alpha; Tables 4 and 5). This protein together with Ig-beta is necessary for the expression and function of the B-cell antigen receptor (BCR). Binding of an antigen to the BCR brings about antigen-BCR endocytosis, its processing, and the resulting peptides being loaded onto MHC class II genes (MHCII) for presentation to CD4 T-cells. Thus, *CD79A* functions may be related to bone loss from OVX according to the hypothesis proposed previously. Indeed, Pacifici [59] proposed that among the mechanisms responsible for OVX-induced bone loss, there is an expansion in the bone marrow of activated T-cells that produce TNF. This is the result of an expansion of mature T-cells in the periphery, which is a consequence of an increase in antigen presentation from the increased expression of MHCII. This, in turn, is driven by a complex mechanism that involves an increased production of IFN-γ and IL-7, a blunted production of TGF-β in bone marrow, and an increase in oxidative stress [59]. One possibility could be that the variants described in the present paper, *e.g.*, the rs1428922 SNP located in 5′ near of *CD79A* gene or other variants in linkage disequilibrium, may cause changes in the expression of the *CD79A* gene. This, consequently, alters parameters related with the activation or presentation processes of these antigen presenting cells (APCs) that confer differential susceptibility to osteoporosis. That notwithstanding, in the future it will be necessary to perform both a gene-wide association study, increasing the number of SNPs, as well as a functional analysis of the SNPs shown to be associated.

Limitations and potential biases of the present study

Our study has some limitations. We used whole bone marrow to compare global gene expression between OVX and SHAM mice instead of isolating a particular cell type, *e.g.*, osteoblasts. Our aim, by designing the experiment in this way, was to minimize the steps between animal sacrifice and the obtention of RNA in order to obtain high quality RNA. Moreover, the animals were sacrificed one month after OVX when the main changes that affect bone metabolism had already occurred. By that time, there are also other changes previously described by us [32,33]. The reason for not choosing the first post-OVX days was to avoid changes in gene expression due to surgery inflammation. Moreover, the model is more similar to women's lives 5–10 years after menopause. There are other limitations. The study included Caucasian postmenopausal women so it is unclear whether the results can be extrapolated to women of a different ethnicity or to men. Additionally, the sample size was medium, although with good statistical power. Moreover, the design of the study was clinical and volunteer based, not population based. Finally, we have no information about participant dietary habits and physical activity.

To avoid false positives in our association study, we analyzed a population of a particular geographic region, having discarded substructures and women of other ancestry, and we have used covariates in the statistical analysis and a multiple test-corrected threshold for statistical significance to diminish the error type I risk related to the multiple SNPs analyzed. Therefore, although we tried to avoid potential biases, some may remain. Further studies with a prospective design and in other cohorts are needed to clarify these issues and to assess the real importance of our findings.

Conclusion

In conclusion, the present study presents a translational approach to the study of genes. It can be used as a tool in the search and identification of new genes associated with osteoporosis in complement with expensive GWAS. We have successfully validated this methodological approach by translating the study of variants in genes *GPX3* and *CD79A* with the bone phenotypes in our cohort of postmenopausal women. Our findings in the association study reinforce the role of antioxidant pathways and of B-cell function in bone homeostasis. This reinforces the need to further study genes of these systems and their relation to postmenopausal osteoporosis.

Supplementary data to this article can be found online at http://dx.doi.org/10.1016/j.bone.2014.05.001.

Acknowledgments

The authors are indebted to Mrs. R. Aliaga for their excellent technical assistance. This work was supported by grants PI09/0184 and PI12/02582 from the Fondo de Investigación Sanitaria (FIS, Madrid, Spain), including funds from FEDER Program from EU. Layla Panach is a predoctoral fellow from the Ministerio de Educación, Cultura y Deporte (Programa de Formación del Profesorado Universitario).

Authors' roles: Study design: MAG-P and BP. Study conduct: BP, IN, ES, AL-F, JJT, CH, AC, and MAG-P. Data collection: BP, ES, IN,

AL-F, LP, and MAG-P. Data analysis: AL-F, ES, JJT, BP, CH, AC and MAG-P. Data interpretation: BP, ES, AL-F, LP, AC, CH, JJT, and MAG-P. Drafting or critically revising the manuscript: BP, ES, AL-F, IN, LP, CH, JJT, AC and MAG-P. All authors approved the final version of manuscript to be published.

Disclosures

All authors state that they have no conflicts of interest.

References

[1] Kanis JA, Burlet N, Cooper C, Delmas PD, Reginster JY, Borgstrom F, et al. European guidance for the diagnosis and management of osteoporosis in postmenopausal women. Osteoporos Int 2008;19:399–428.
[2] Kanis JA, Oden A, Johnell O, Johansson H, De Laet C, Brown J, et al. The use of clinical risk factors enhances the performance of BMD in the prediction of hip and osteoporotic fractures in men and women. Osteoporos Int 2007;18:1033–46.
[3] Delgado-Calle J, Garmilla P, Riancho JA. Do epigenetic marks govern bone mass and homeostasis? Curr Genomics 2012;13:252–63.
[4] Ralston SH, Uitterlinden AG. Genetics of osteoporosis. Endocr Rev 2010;31:629–62.
[5] Peacock M, Turner CH, Econs MJ, Foroud T. Genetics of osteoporosis. Endocr Rev 2002;23:303–26.
[6] Ralston SH, de Crombrugghe B. Genetic regulation of bone mass and susceptibility to osteoporosis. Genes Dev 2006;20:2492–506.
[7] Ioannidis JP, Ng MY, Sham PC, Zintzaras E, Lewis CM, Deng HW, et al. Meta-analysis of genome-wide scans provides evidence for sex- and site-specific regulation of bone mass. J Bone Miner Res 2007;22:173–83.
[8] Styrkarsdottir U, Halldorsson BV, Gretarsdottir S, Gudbjartsson DF, Walters GB, Ingvarsson T, et al. New sequence variants associated with bone mineral density. Nat Genet 2009;41:15–7.
[9] Rivadeneira F, Styrkarsdottir U, Estrada K, Halldorsson BV, Hsu YH, Richards JB, et al. Twenty bone-mineral-density loci identified by large-scale meta-analysis of genome-wide association studies. Nat Genet 2009;41:1199–206.
[10] Uitterlinden AG, van Meurs JB, Rivadeneira F, Pols HA. Identifying genetic risk factors for osteoporosis. J Musculoskelet Neuronal Interact 2006;6:16–26.
[11] Estrada K, Styrkarsdottir U, Evangelou E, Hsu YH, Duncan EL, Ntzani EE, et al. Genome-wide meta-analysis identifies 56 bone mineral density loci and reveals 14 loci associated with risk of fracture. Nat Genet 2012;44:491–501.
[12] Hsu YH, Kiel DP. Clinical review: genome-wide association studies of skeletal phenotypes: what we have learned and where we are headed. J Clin Endocrinol Metab 2012;97:E1958–77.
[13] Richards JB, Rivadeneira F, Inouye M, Pastinen TM, Soranzo N, Wilson SG, et al. Bone mineral density, osteoporosis, and osteoporotic fractures: a genome-wide association study. Lancet 2008;371:1505–12.
[14] Riggs BL, Khosla S, Melton III LJ. A unitary model for involutional osteoporosis: estrogen deficiency causes both type I and type II osteoporosis in postmenopausal women and contributes to bone loss in aging men. J Bone Miner Res 1998;13:763–73.
[15] Cano A, Dapia S, Noguera I, Pineda B, Hermenegildo C, del Val R, et al. Comparative effects of 17beta-estradiol, raloxifene and genistein on bone 3D microarchitecture and volumetric bone mineral density in the ovariectomized mice. Osteoporos Int 2008;19:793–800.
[16] Cenci S, Weitzmann MN, Roggia C, Namba N, Novack D, Woodring J, et al. Estrogen deficiency induces bone loss by enhancing T-cell production of TNF-alpha. J Clin Invest 2000;106:1229–37.
[17] Kendziorski CM, Zhang Y, Lan H, Attie AD. The efficiency of pooling mRNA in microarray experiments. Biostatistics 2003;4:465–77.
[18] Sobrino A, Oviedo PJ, Novella S, Laguna-Fernandez A, Bueno C, García-Pérez MA, et al. Estradiol stimulates vasodilatory and metabolic pathways in cultured human endothelial cells. Mol Cell Endocrinol 2011;335:96–103.
[19] Tarraga J, Medina I, Carbonell J, Huerta-Cepas J, Minguez P, Alloza E, et al. GEPAS, a web-based tool for microarray data analysis and interpretation. Nucleic Acids Res 2008;36:W308–14.
[20] Pineda B, Hermenegildo C, Tarin JJ, Laporta P, Cano A, Garcia-Perez MA. Alleles and haplotypes of the estrogen receptor alpha gene are associated with an increased risk of spontaneous abortion. Fertil Steril 2010;93:1809–15.
[21] Pineda B, Hermenegildo C, Laporta P, Tarin JJ, Cano A, Garcia-Perez MA. Common polymorphisms rather than rare genetic variants of the Runx2 gene are associated with femoral neck BMD in Spanish women. J Bone Miner Metab 2010;28:696–705.
[22] Pineda B, Tarin JJ, Hermenegildo C, Laporta P, Cano A, Garcia-Perez MA. Gene–gene interaction between CD40 and CD40L reduces bone mineral density and increases osteoporosis risk in women. Osteoporos Int 2011;22:1451–8.
[23] Li H, Cuartas E, Cui W, Choi Y, Crawford TD, Ke HZ, et al. IL-1 receptor-associated kinase M is a central regulator of osteoclast differentiation and activation. J Exp Med 2005;201:1169–77.
[24] Hartgring SA, van Roon JA, Wenting-van WM, Jacobs KM, Jahangier ZN, Willis CR, et al. Elevated expression of interleukin-7 receptor in inflamed joints mediates interleukin-7-induced immune activation in rheumatoid arthritis. Arthritis Rheum 2009;60:2595–605.
[25] Sakamoto W, Isomura H, Fujie K, Iizuka T, Nishihira J, Tatebe G, et al. The effect of vitamin K2 on bone metabolism in aged female rats. Osteoporos Int 2005;16:1604–10.
[26] Barrett JC, Fry B, Maller J, Daly MJ. Haploview: analysis and visualization of LD and haplotype maps. Bioinformatics 2005;21:263–5.
[27] Sole X, Guino E, Valls J, Iniesta R, Moreno V. SNPStats: a web tool for the analysis of association studies. Bioinformatics 2006;22:1928–9.
[28] Pritchard JK, Stephens M, Donnelly P. Inference of population structure using multilocus genotype data. Genetics 2000;155:945–59.
[29] Nyholt DR. A simple correction for multiple testing for single-nucleotide polymorphisms in linkage disequilibrium with each other. Am J Hum Genet 2004;74:765–9.
[30] Gauderman WJ. Sample size requirements for association studies of gene–gene interaction. Am J Epidemiol 2002;155:478–84.
[31] Manolio TA, Collins FS, Cox NJ, Goldstein DB, Hindorff LA, Hunter DJ, et al. Finding the missing heritability of complex diseases. Nature 2009;461:747–53.
[32] Garcia-Perez MA, del Val R, Noguera I, Hermenegildo C, Pineda B, Martinez-Romero A, et al. Estrogen receptor agonists and immune system in ovariectomized mice. Int J Immunopathol Pharmacol 2006;19:807–19.
[33] Garcia-Perez MA, Noguera I, Hermenegildo C, Martinez-Romero A, Tarin JJ, Cano A. Alterations in the phenotype and function of immune cells in ovariectomy-induced osteopenic mice. Hum Reprod 2006;21:880–7.
[34] Xiao Y, Fu H, Prasadam I, Yang YC, Hollinger JO. Gene expression profiling of bone marrow stromal cells from juvenile, adult, aged and osteoporotic rats: with an emphasis on osteoporosis. Bone 2007;40:700–15.
[35] Masuzawa T, Miyaura C, Onoe Y, Kusano K, Ohta H, Nozawa S, et al. Estrogen deficiency stimulates B lymphopoiesis in mouse bone marrow. J Clin Invest 1994;94:1090–7.
[36] Miyaura C, Onoe Y, Inada M, Maki K, Ikuta K, Ito M, et al. Increased B-lymphopoiesis by interleukin 7 induces bone loss in mice with intact ovarian function: similarity to estrogen deficiency. Proc Natl Acad Sci U S A 1997;94:9360–5.
[37] Han X, Kawai T, Eastcott JW, Taubman MA. Bacterial-responsive B lymphocytes induce periodontal bone resorption. J Immunol 2006;176:625–31.
[38] Toraldo G, Roggia C, Qian WP, Pacifici R, Weitzmann MN. IL-7 induces bone loss in vivo by induction of receptor activator of nuclear factor kappa B ligand and tumor necrosis factor alpha from T cells. Proc Natl Acad Sci U S A 2003;100:125–30.
[39] Wheater G, Hogan VE, Teng YK, Tekstra J, Lafeber FP, Huizinga TW, et al. Suppression of bone turnover by B-cell depletion in patients with rheumatoid arthritis. Osteoporos Int 2011;22:3067–72.
[40] Li Y, Li A, Yang X, Weitzmann MN. Ovariectomy-induced bone loss occurs independently of B cells. J Cell Biochem 2007;100:1370–5.
[41] Li Y, Toraldo G, Li A, Yang X, Zhang H, Qian WP, et al. B cells and T cells are critical for the preservation of bone homeostasis and attainment of peak bone mass in vivo. Blood 2007;109:3839–48.
[42] Weitzmann MN, Roggia C, Toraldo G, Weitzmann L, Pacifici R. Increased production of IL-7 uncouples bone formation from bone resorption during estrogen deficiency. J Clin Invest 2002;110:1643–50.
[43] Horowitz MC, Fretz JA, Lorenzo JA. How B cells influence bone biology in health and disease. Bone 2010;47:472–9.
[44] Li JY, Tawfeek H, Bedi B, Yang X, Adams J, Gao KY, et al. Ovariectomy disregulates osteoblast and osteoclast formation through the T-cell receptor CD40 ligand. Proc Natl Acad Sci U S A 2011;108:768–73.
[45] Shinohara M, Koga T, Okamoto K, Sakaguchi S, Arai K, Yasuda H, et al. Tyrosine kinases Btk and Tec regulate osteoclast differentiation by linking RANK and ITAM signals. Cell 2008;132:794–806.
[46] Kiviranta R, Yamana K, Saito H, Ho DK, Laine J, Tarkkonen K, et al. Coordinated transcriptional regulation of bone homeostasis by Ebf1 and Zfp521 in both mesenchymal and hematopoietic lineages. J Exp Med 2013;210:969–85.
[47] Cremasco V, Decker CE, Stumpo D, Blackshear PJ, Nakayama KI, Nakayama K, et al. Protein kinase C-delta deficiency perturbs bone homeostasis by selective uncoupling of cathepsin K secretion and ruffled border formation in osteoclasts. J Bone Miner Res 2012;27:2452–63.
[48] Duncan EL, Danoy P, Kemp JP, Leo PJ, McCloskey E, Nicholson GC, et al. Genome-wide association study using extreme truncate selection identifies novel genes affecting bone mineral density and fracture risk. PLoS Genet 2011;7:e1001372.
[49] Edwards JC, Cohen C, Xu W, Schlesinger PH. c-Src control of chloride channel support for osteoclast HCl transport and bone resorption. J Biol Chem 2006;281:28011–22.
[50] Zhang Z, Shively JE. Acceleration of bone repair in NOD/SCID mice by human monoosteophils, novel LL-37-activated monocytes. PLoS One 2013;8:e67649.
[51] Hojo H, Ohba S, Taniguchi K, Shirai M, Yano F, Saito T, et al. Hedgehog-Gli activators direct osteo-chondrogenic function of bone morphogenetic protein toward osteogenesis in the perichondrium. J Biol Chem 2013;288:9924–32.
[52] Kyle KA, Willett TL, Baggio LL, Drucker DJ, Grynpas MD. Differential effects of PPAR-{gamma} activation versus chemical or genetic reduction of DPP-4 activity on bone quality in mice. Endocrinology 2011;152:457–67.
[53] Seo E, Basu-Roy U, Zavadil J, Basilico C, Mansukhani A. Distinct functions of Sox2 control self-renewal and differentiation in the osteoblast lineage. Mol Cell Biol 2011;31:4593–608.
[54] Le Mellay V, Grosse B, Lieberherr M. Phospholipase C beta and membrane action of calcitriol and estradiol. J Biol Chem 1997;272:11902–7.
[55] Pineda B, Laporta P, Hermenegildo C, Cano A, García-Pérez MA. A C>T polymorphism located at position-1 of the Kozak sequence of *CD40* gene is associated with low bone mass in Spanish postmenopausal women. Osteoporos Int 2008;19:1147–52.
[56] Lopez-Granados E, Temmerman ST, Wu L, Reynolds JC, Follmann D, Liu S, et al. Osteopenia in X-linked hyper-IgM syndrome reveals a regulatory role for CD40 ligand in osteoclastogenesis. Proc Natl Acad Sci U S A 2007;104:5056–61.
[57] Gao Y, Wu X, Terauchi M, Li JY, Grassi F, Galley S, et al. T cells potentiate PTH-induced cortical bone loss through CD40L signaling. Cell Metab 2008;8:132–45.
[58] Manolagas SC. From estrogen-centric to aging and oxidative stress: a revised perspective of the pathogenesis of osteoporosis. Endocr Rev 2010;31:266–300.
[59] Pacifici R. Role of T cells in ovariectomy induced bone loss—revisited. J Bone Miner Res 2012;27:231–9.